Toward Interpreting Failure in Sintered-Silver Interconnection Systems†

M. C. Modugno, A. A. Wereszczak, and S. B. Waters
Oak Ridge National Laboratory, Oak Ridge, TN 37831

Abstract

The mechanical strength and subsequent reliability of a sintered-silver interconnection "system" is a function of numerous independent parameters, and that "system" is still undergoing process development. Most of those parameters (e.g., choice of plating) are arguably and unfortunately often taken for granted and are independent of the silver's cohesive strength. To explore such effects, shear strength testing and failure analyses were completed on a simple, mock sintered-silver interconnection system consisting of bonding two DBC ceramic substrates. Silver and gold platings were part of the test matrix, as were drying strategies, and the consideration of stencil-printing vs. screen-printing. Shear strength of sintered-silver interconnect systems was found to be insensitive to the choice of plating, drying practice, and printing method provided careful and consistent processing of the sintered-silver are practiced. Lastly, with the examined interconnection systems, it was observed that a maximum shear failure stress of ~ 60 MPa is achievable.

Key words: Packaging & Processing

Introduction:

Sintered silver (Ag) has attention as a potential replacement for traditional lead-based and tin-based solders. The material properties of silver allow for electronic devices to operate at significantly higher temperature. Furthermore, high electrical and thermal conductivities lessen localized joule heating and enables more efficient dissipation of thermal energy from the system. An additional benefit to using silver is its compliance with RoHS standards.

Due to its favorable material properties, silver has attractiveness for use in several key interconnect applications in power electronics such as joining die with substrates and substrates with heat sinks. The high thermal conductivity promotes heat transfer from the device to a heat sink where the energy can more easily be dissipated. Devices can be designed to operate at higher temperatures as a result of the use of silver. This makes silver an excellent candidate as a die attach material for wide band gap semiconductors such as silicon carbide.

A major consideration when choosing a joining material is the ability of said material to create a strong bond between the mating surfaces. Increased attention of late has been directed towards the mechanical reliability of sintered-Ag interconnects [1-11].

Experimental Approach:

The purpose of this effort is to determine and interpret how several processing parameters affect the mechanical response of sinterable silver interconnect systems. Three independent parameters were varied: plating material, printing method, and effect of pre-drying paste prior to sample assembly. Mock interconnect systems were created by bonding two similarly plated direct bonded copper (DBC) substrates to one another with sinterable Ag. The bonding of two DBC substrates was chosen as a

Notice: This manuscript has been authored by UT-Battelle, LLC under Contract No. DE-AC05-00OR22725 with the U.S. Department of Energy. The United States Government retains and the publisher, by accepting the article for publication, acknowledges that the United States Government retains a non-exclusive, paid-up, irrevocable, world-wide license to publish or reproduce the published form of this manuscript, or allow others to do so, for United States Government purposes. The Department of Energy will provide public access to these results of federally sponsored research in accordance with the DOE Public Access Plan (http://energy.gov/downloads/doe-public-access-plan).

simplified system that facilitates shear testing; if a brittle and fragile die serves as the means of applying shear to its bonded interconnect, then it invariably fractures before complete evaluation of that interconnect can occur. A total of twelve test groups, each containing 12 samples, were examined.

Sample Preparation

Samples were processed using a HMI Presco 485 screen printer. Approximately 20 psi (140 kPa) of pressure was applied to the squeegee as it traveled 1.63 in/s (4.14 cm/s) depositing Loctite Ablestik SSP 2020 (Henkel) Ag paste, onto a 12.7 x 12.7 x 1.2 mm gold (Au) or Ag plated DBC substrate (Remtec/Rogers/Curamik). A print pattern similar to the pattern on a 5-count dice (shown in Fig. 1) was used in order to help distribute the stress across the plated DBC substrate. This symmetric pattern also helped to keep both the DBC substrates parallel to one another during sample assembly. Furthermore, a circular geometry was desired in order to avoid creating regions of high stress intensity caused by edges (e.g., such that results when using squares). The total bonded area for all specimens is 20 mm^2. The print pattern was centered on clean DBC substrates.

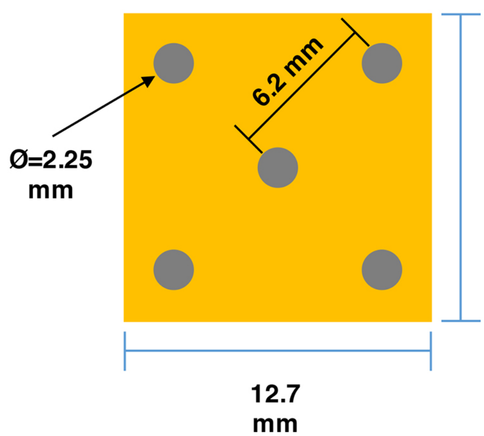

Figure 1. Schematic displaying print pattern and dimensions (not drawn to scale).

Each printing method created different thicknesses of sintered pads. Pad thickness is directly related to the thickness of the stencil or screen used and were 100 μm (4 mils) and 15 μm (0.6 mils), respectively. Furthermore, the employed screen was 170 U.S. standard mesh with a squeegee angle of 45°. Table I shows the post-sintering thickness for each processing method.

Table I: Average post-sintering bond thicknesses.

Processing Method	Stencil Printed Bond Thickness (μm)	Screen Printed Bond Thickness (μm)
Dry	85	25
Wet Low Stress	25	15
Wet High Stress	20	15

Following printing, a second plated DBC substrate was set onto the printed Ag creating a "DBC-sandwich". Throughout this paper "wet-processed samples" refers to those DBC substrates that were mated while the paste was still wet whereas "dry-processed samples" refer to those that were open-exposure pre-dried prior to sample mating. The following provides additional details of the processing conditions:

- Dry processed: Dry-processed samples were dried at 50°C for 30 minutes in air before an equally sized and plated substrate was set onto the printed paste.
- Wet high stress processed: Sample assembly was performed prior to drying in the case of wet processed samples. These samples were dried at 50°C for 30 minutes in air while the dead weight of the sintering fixture imparted a uniaxial compressive stress of 0.17 MPa. These samples are referred to as wet high stress processed (WetHS).
- Wet low stress processed: A second group of wet processed samples were created in which a uniaxial compressive stress of 0.01 MPa was applied to the samples during drying. These samples are referred to as wet low stress processed (WetLS).

The DBC sandwiches were then sintered upon completion of drying and assembly. A total of 12 samples were loaded into a custom sintering fixture comprised of 3 alignment columns each containing 4 stacks of DBC sandwiches. The sintering fixture was then placed into an Instron SFL sintering oven mounted within an Applied Test Systems dead weight frame that applied uniaxial compression during sintering. Samples were sintered at 250°C for 1 hr under an applied stress of 3 MPa. At the end of the sintering cycle samples were allowed to cool naturally to 100°C before the oven door was opened in order to increase the rate of cooling. Cooling occurred while the samples were still compressed. Specimen position in the fixture was kept track of.

Mechanical Testing

Force at failure was determined using a Nordson Dage Series 4000 Bondtester via uniaxially applied shear loading. The shear tool was actively aligned to the edge of the coupon before each test's commencement. The stage, containing the (lower DBC) fixed sample, was set to a constant displacement rate of 25 μm/s with the shear tool at a fixed height of 750 μm off the stage allowing the force to be solely applied to the upper DBC substrate. Markings were placed on the upper and lower DBC substrates so that the direction of applied force could be traceable. Also, the DBC substrate that had been set into the printed paste was consistently in contact with the shear tool. The measured force at failure was divided by the bond area to calculate the shear failure stress.

Failure Analysis

A portion of the failure analysis consisted of optical microscopy performed on the failed surfaces using a Nikon SMZ1500 stereo microscope. Samples from each test group were ranked according to their corresponding failure stress, and were visually analyzed in ascending order, and all were examined twice. During the second observation session sketches were made of the failed surfaces to aid in drawing conclusions about various failure types. Images were taken of the failed surfaces in order to correct pad area for the stress at failure calculations.

The remaining failure analysis was done using a scanning electron microscopy (SEM, Hitachi S-4800) with the use of energy dispersive spectroscopy (EDS) to determine chemistries whose interpretation supported the determination of failure mechanism or failure type.

Strength Data Interpretation

Shear strength data was regressed against a two-parameter Weibull distribution and the distribution for each of the independent parameters were interpreted and compared. This analysis also aided in the graphical identification of the activity of multiple strength-limiting populations. Weibull plots often show a monomodal distribution. However, there are often two or more distributions present, and their interpretation can provide insights about operative and discrete flaw types, and any potential processing and testing parasitics.

Parametric Evaluation

Potential interdependencies of the independent parameters were examined. For example, linking the processing methods to the platings allowed for identification of any potential constructive, destructive, or benign pairings.

Results and Discussion:

The scatter for the shear failure stresses are shown in Fig. 2 for each of the 12 test groups. The majority could withstand at least 20 MPa of uniaxial applied shear stress but all failed at shear stresses greater than 60 MPa. There were varying degrees of variance within each test group. The calculated shear stresses necessary to cause failure were greater than or equal to those reported values in references 1-11.

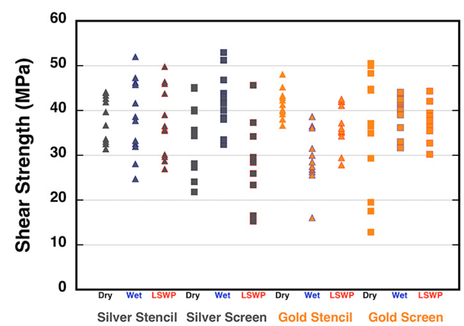

Figure 2. Shear stress at failure for all test groups.

In the following subsections the shear strength results are parametrically evaluated in context to this study's three primary independent conditions.

Plating

A major consideration for designing power electronic devices is choosing requisite plating. Common plating materials, including Ag and Au, allow for bonding between the substrate and die, and between substrate and baseplate or heat-sink. The effect of Ag and Au metallization on the shear strength of the examined DBC sandwiches is shown in Fig. 3. For applied shear stresses greater than ~ 25 MPa, their distributions were quite similar.

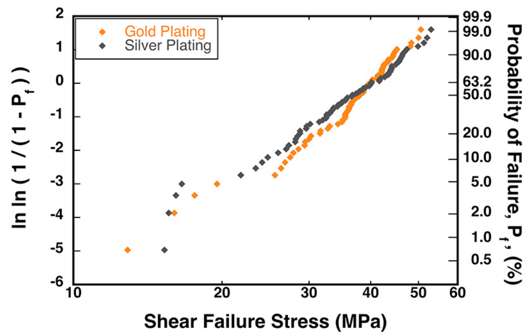

Figure 3. Weibull plot comparing shear stress at failure to plating material.

To further explore the reliability of Au platings, their data were plotted against printing and drying techniques. This is shown in Fig. 4. This portrayal provides evidence that the combination of dry processing and screen printing have the potential to create failures at relatively low shear stresses.

There is graphical evidence of two or more exclusive flaw populations in Fig. 4 (a) and (b) when each test group is individually observed. This indicates that processing or testing inconsistencies or both occurred. The presence of exclusivity is a sign that the employed process or testing or both require additional development.

The cause of these relatively low shear failure strengths associated with exclusive flaw populations deserved attention. The silver paste is forced through a fine mesh screen during screen printing. This results in an egg-carton like texture being imparted onto the surface of the substrate as the screen rebounds. When the paste is dried prior to setting the companion substrate, that egg-carton-like structure is sustained but becomes stiffer because its dryness and its structure may not collapse under the compressive loading used during sintering. This structure is then visible post-mechanical testing suggesting its structure can serve as a contributing cause of lower-strength shear failure.

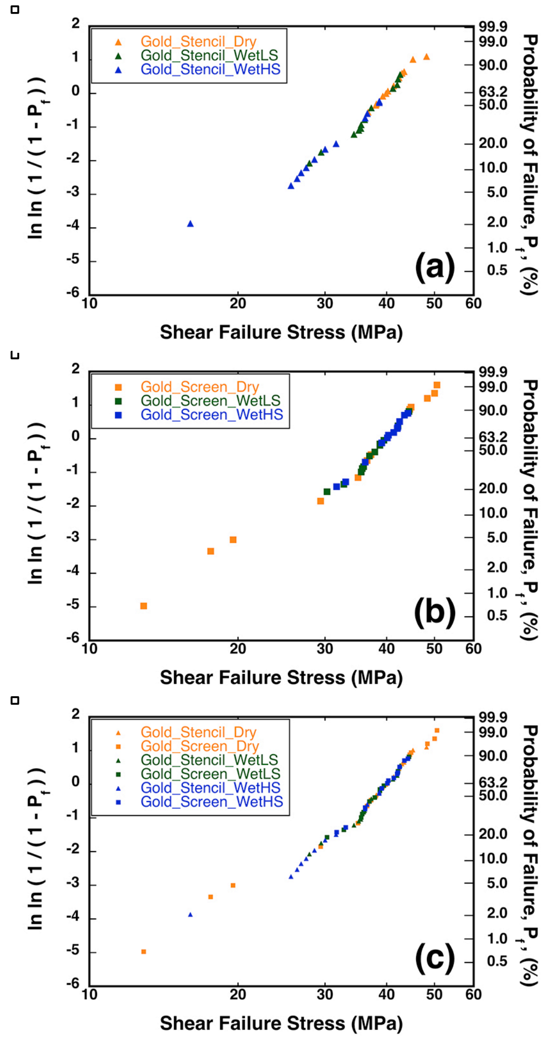

Figure 4. Weibull plots showing shear failure stresses for Au plated DBC substrates that used (a) stencil printing (b) screen printing and (c) combined. Data is separated to discriminate printing and drying techniques.

A discrete failure mechanism appears to be associated with wetHS processing. Failure analysis showed there was a significant increase in bond area that is linked to plastic deformation that had occurred in the paste prior to its thorough drying. The authors speculate that microstructural changes had occurred in the sintered silver due to that pre-drying deformation and that that ultimately lessened the ability of the final sintered silver to sustain relatively high shear stresses.

Equivalent parametric evaluation was performed on shear strength data for the silver-plated sets, and that is represented in Fig. 5. The majority of the data (i.e., all data > 20 MPa) fits a monomodal distribution with the exception of four outliers that portray exclusivity. Those outliers are linked to samples associated with the combination of the wetLS processing method and screen printing. Further pedigree tracing back to the processing revealed that the four samples were sintered in the same run. Therefore, some parasitic issue likely occurred during sintering that manifested itself into this exclusivity and relatively low shear failure stresses for these specimens.

Energy dispersive spectroscopy images of sectioned Au and Ag plated DBC substrates are shown in Figs. 6 and 7, respectively. In order to deposit a Au plating onto the DBC substrate's copper cladding, a nickel-phosphorous (Ni-P) interlayer was used. This means that failure could have hypothetically occurred at 8 different locations in this Au-plating-containing interconnect system: adhesive failure between the sintered-Ag and Au plating, between the Au plating and Ni-P interlayer, between the Ni-P interlayer and DBC's copper cladding, or between the DBC's copper cladding and the alumina (Al_2O_3) dielectric, or cohesive failure within the sintered-Ag, within the Au plating, within the Ni-P interlayer, or within the Al_2O_3 dielectric substrate.

The Ag-plating is able to be directly bonded to the DBC's copper cladding. Therefore, the plated DBC substrate consists of 3 layer allowing for failure to hypothetically occur at 7 different locations with this Ag-plating-containing interconnect system: adhesive failure between the sintered-Ag and Ag plating, Ag plating and DBC's copper cladding, DBC copper cladding and the Al_2O_3 substrate, or cohesively in the sintered-Ag, Ag plating, DBC copper cladding, or Al_2O_3 substrate.

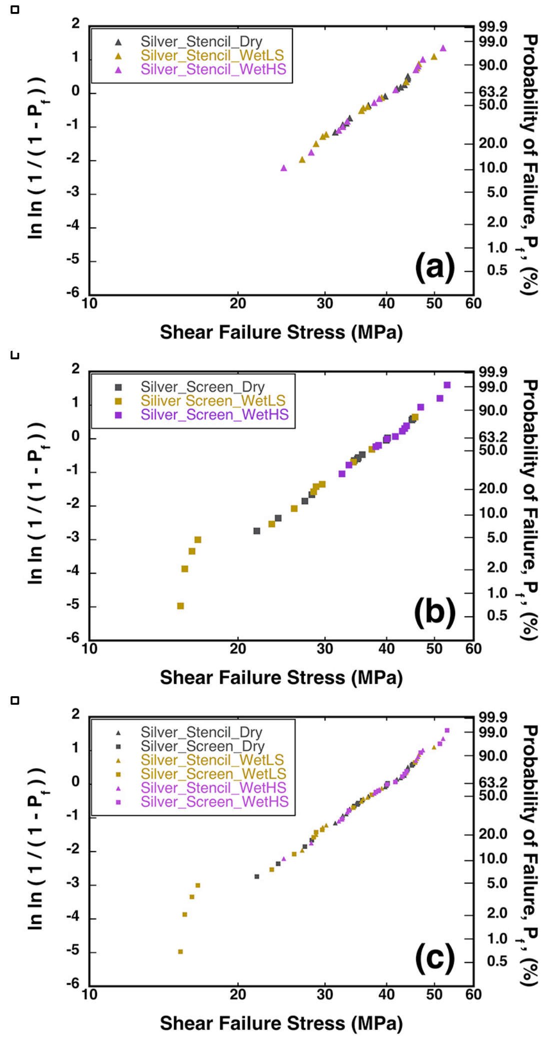

Figure 5. Weibull plots showing shear failure stresses for silver-plated DBC substrates that used (a) stencil printing (b) screen printing and (c) combined. Data is further separated to discriminate among printing and drying techniques.

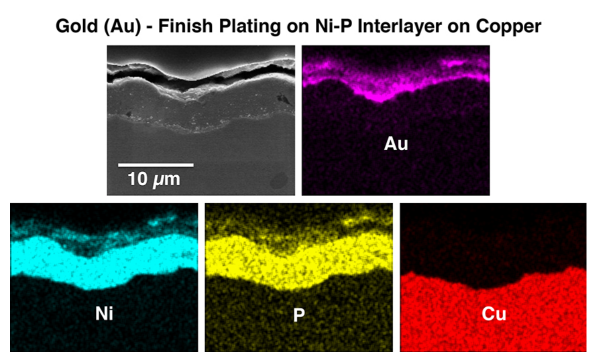

Figure 6. EDS elemental map showing the gold plating with the Ni-P sub-layer bound to the DBC.

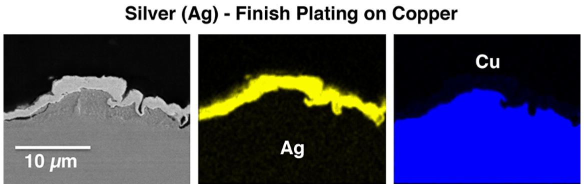

Figure 7. EDS elemental map showing the Ag plating bound to the DBC.

The plating material's impact on how the DBC sandwiches failed were observed through the use of optical microscopy and EDS. Gold-plated DBC substrates tended to fail cohesively with minor amounts of adhesive failure between the sintered-Ag and Au plating. There is also a small amount of adhesive failure between the Au plating and Ni-P sub-layer as shown in Fig. 8.

The typical location of failure for Ag plated DBC substrates (both for screen and stencil printed samples) is shown in Fig. 9. The DBC sandwiches tend to fail adhesively between the Ag plating and the DBC-cladding. This observation suggests that the weakest part of the entire interconnect system is at this interface.

There was evidence of some form of plating failure for all specimens. This suggests that the strength of sintered-Ag interconnect systems, at least for the systems explored in this study, is limited to the adhesive strength of the plating being used. Interestingly, even though the two platings used in this study failed differently, all specimen failed at under similar shear stresses.

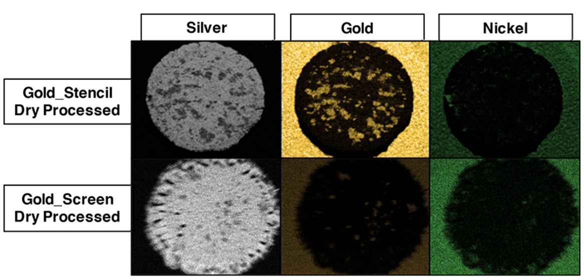

Figure 8. EDS elemental mapping of a typical Au plated surface (post testing). Images are provided for both screen and stencil printed samples.

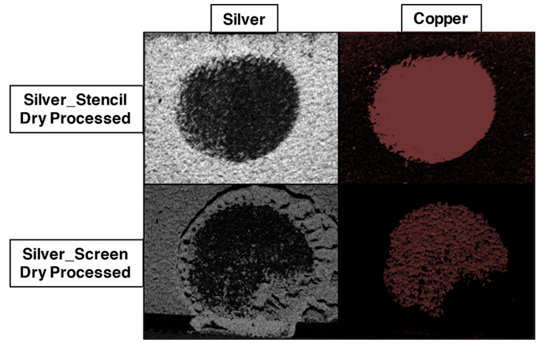

Figure 9. EDS elemental mapping of a typical Ag plated surface (post testing). Images are provided for both screen and stencil printed samples.

Processing Method

In recent years there has been a call to remove the pre-drying stage by combining assembly, drying, and sintering into one continuous process. This requires the assembly of the device to occur when the paste is still wet and is referred to in this paper as wet processing. Originally, the authors planned to solely address dry and wetHS processing; however, during failure analysis it was discovered that there was a substantial increase in the bond area of the wetHS processed samples. Therefore, a third processing method, designated here as wetLS processing, was implemented in which less stress was applied to the samples during drying.

Shear strength data suggests that there is a minimal effect of processing method on the shear strength. This is shown in Fig. 10. All three processing techniques create samples that exhibited a similar Weibull distribution, and minimum and maximum shear strengths. However, failure analysis indicated cause for concern when using either of the wet processing techniques; namely, there is greater sensitivity of the resulting shear strength when using the wet process.

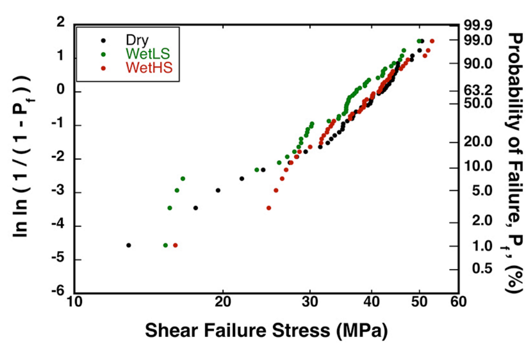

Figure 10. Shear failure stress data for the three drying methods.

The increase in bond area mentioned above for wet processed samples continues to occur even when a low stress (0.01 MPa) was concurrently applied during drying. This phenomenon requires further attention when the final size of the interconnect is critical to the application. The decrease in exposed surface area due to the presence of the mating surface is decreasing the drying rate and its efficacy too; therefore, at the end of the prescribed drying schedule there is adequate plasticity in the paste to cause permanent deformation once there is an increase in applied stress during sintering.

Printing Technique

The strength benefits of either using screen or stencil printing were determined by comparing their produced shear failure stress distributions. The similar Weibull distributions shown in Figs. 11 for both stencil and screen printed specimen indicated printing-technique insensitivity. At shear stresses below 30 MPa the strength-limiting flaw appears to be associated with the choice of processing technique. Figures 12(a)-(b) show parametric comparisons for stencil and screen printed specimens. The distribution suggests that wet processing can introduce additional failure mechanisms that lessen the shear failure stress for stencil printed samples. The strength of screen printed specimen are limited by dry processing due to the inability to break down the egg-carton texture that results from printing.

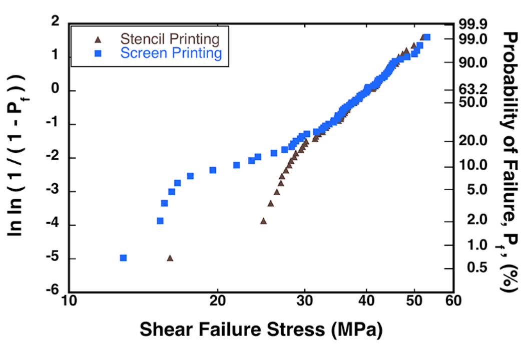

Figure 11. Shear failure stress data for the two printing methods.

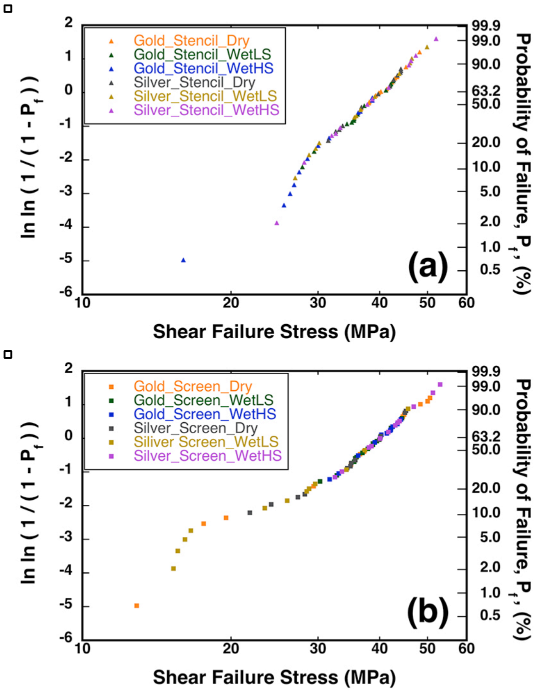

Figure 12. Shear failure stress data for the two printing method but discriminated by (a) stencil and (b) screen printing.

Conclusions:

- Shear strength of the explored sinterable-silver interconnect system was insensitive to the choice of:
  - gold or silver as platings,
  - processing method (pre-drying vs. wet-surface-consolidation), and
  - printing method.
- Despite shear strength being insensitive to the processing method, compromised print-pad structure can be introduced with pre-dried screen-printed and wet-processed sinterable-silver, and that can manifest itself into relatively low shear strength of the interconnects.
- Silver-plated DBC sandwiches tended to adhesively fail between the Ag plating and DBC cladding.
- Gold-plated DBC sandwiches tended to fail in a hybrid manner with the majority of failure resulting from cohesive failure of the sintered-Ag bond with additional adhesive failure between the Au plating and the Ni-P sub-layer.

- Sintered-Ag interconnect systems should be able to withstand shear stresses of ~30 MPa if consistent processing (i.e. no exclusive flaw types) is employed. They will fail if service shear stresses exceed ~ 60 MPa.
- Because sinterable-silver is still undergoing process development, the employment of combined Weibull and failure analysis can be useful in identifying exclusivity and parasitics associated with its process development and testing or both.

Acknowledgments

Research co-sponsored by the Propulsion Materials Program and the Electric Drive Technologies Programs, DOE Vehicle Technologies Office, under contract DE-AC05-00OR22725 with UT-Battelle, LLC.

The authors thank USDOE's J. Gibbs and S. Rogers, ORNL's A. Haynes and B. Ozpineci for their programmatic support, ORNL's B. Armstrong, R. Wiles, C. Ayers, and S. Campbell for their technical support, and ORNL's B. Ozpineci and Z. Liang for reviewing the manuscript.

References

[1] W. Tao, X. Chen, G. Lu, and G. Lei, "Low Temperature Sintering with Nano-Silver Paste in Die Attached Interconnection." *Journal of Electronic Materials* 36, no. 10 (2007): 1333-1340.

[2] Q. Kun, X. Chen, and G. Lu, "Effect of Interconnection Area on the Shear Strength of Sintered Joint with Nano-Silver Paste." *Soldering and Surface Mount Technology* 20 (2008): 8-12.

[3] Y.Morisada, T. Nagaoka, M. Fukusumi, Y. Kashiwagi, M. Yamamoto, and M. Nakamoto, "A Low-Temperature Bonding Process Using Mixed Cu-Ag Nanoparticles." *Journal of Electronic Materials* 39, no. 8 (2010): 1283-1288.

[4] L. Xin, G. Chen, X. Chen, G. Lu, L. Wang, and Y. Mei, "Mechanical Property Evaluation of Nano-Silver Paste Sintered Joint using Lap-Shear Test." *Soldering and Surface Mount Technology* 24, no. 2 (2012): 120-126.

[5] F. Le Henaff, S. Azzopardi, J. Deletage, E. Woirgard, S. Bontemps, and J. Joguet, "A Preliminary Study on the Thermal and Mechanical Preformances of Sintered Nano-Scale Silver Die-Attach Technology Depending on the Substrate Metalization." *Microelectronics Reliability* 52 (2012): 2321-2325.

[6] T. Yansong, X. Li, and X. Chen, "Fatigue and Dwell-Fatigue Behavior of Nano-Silver Sintered Lap-Shear Joint at Elevated Temperature." *Microelectronic Reliability* 54 (2014): 648-653.

[7] L. Mingyu, Y. Xiao, Z. Zhang, and J. Yu, "Bimodal Sintered Silver Nanoparticle Paste with Ultrahigh Thermal Conductivity and Shear Strength for High Temperature Thermal Interface Material Applications." *ACS Appl. Mater. Interfaces* 7 (2015): 9157-9168.

[8] R. Khazaka, L. Mendizabal, and D. Henry. "Review on Joint Shear Strength of Nano-Silver Paste and Its Long_Term High Temperature Reliability." *Journal of Electronic Materials* 43, no. 7 (2014): 2459-2466.

[9] S. Kim. "Mechanical Properties of Nano-Silver Joints as Die Attach Materials." *Journal of Alloys and Compounds* 514 (2012): 6-19.

[10] A. A. Wereszczak, Z. Liang, M. K. Ferber, and L. D. Marlino, "Uniqueness and Challenges of Sintered Silver as a Bonded Interface Material," *Journal of Microelectronics and Electronic Packaging*, 11:158-165 (2014).

[11] ORNL/TM-2012/130 Report: "Properties of Bulk Sintered Silver as a Function of Porosity," A. A. Wereszczak, D. J. Vuono, H. Wang, M. K. Ferber, and Z. Liang, June, 2012.

[12] ASTM Standard C1239, 2013, "Standard Practice for Reporting Uniaxial Strength Data and Estimating Weibull Distribution Parameters for Advanced Ceramics," ASTM International, West Conshohocken, PA, 2003.